A&A 468, 19–23 (2007)
DOI: 10.1051/0004-6361:20064818

Astronomy & Astrophysics

Mass variance and cluster abundance in the context of a Gaussian + lognormal distribution model

A. L. B. Ribeiro[1], C. M. Coelho[1,2], A. P. A. Andrade[1], and M. S. Dantas[1,3]

[1] Laboratório de Astrofísica Teórica e Observacional, Departamento de Ciências Exatas e Tecnológicas, Universidade Estadual de Santa Cruz – 45650-000, Ilhéus, Brazil
e-mail: [albr;apaula]@uesc.br
[2] Instituto Nacional de Pesquisas Espaciais, Divisão de Astrofísica – CP 515, 12245-970, São José dos Campos, SP, Brazil
e-mail: carla@das.inpe.br
[3] Instituto Nacional de Pesquisas Espaciais, Laboratório Associado de Computação e Matemática Aplicada – CP 515, 12245-970, São José dos Campos, SP, Brazil
e-mail: msdantas@lac.inpe.br

Received 5 January 2006 / Accepted 5 February 2007

ABSTRACT

Context. We investigate the behavior of the mass variance and the mass function of galaxy clusters in a mixed distribution model.
Aims. Our aim is to find a relation between the mass variance at a 8 h^{-1} Mpc scale, σ_8, and the parameter controlling the Gaussian deviation in the model, α_0, and to constrain the non-Gaussianity using observational data at cluster scales.
Methods. By assuming that the statistics of the density field is built as a weighted mixture of two components, a Gaussian + Lognormal distribution, we rewrite the mass variance expression and the mass function for galaxy clusters.
Results. We find a relation between the mass variance at a 8 h^{-1} Mpc scale, σ_8, and the scale parameter controlling the Gaussian deviation in the model, α_0. This result, in conjunction with observational constraints on the mass variance and high-z galaxy clustering, suggests a scenario where structures develop earlier in comparison to strictly Gaussian models, even for $\alpha_0 \lesssim 0.003$ Mpc. Our model also indicates that only well selected galaxy cluster samples at $z \gtrsim 1$ can discriminate between Gaussian and non-Gaussian (mixed) distribution models.

Key words. cosmological parameters – galaxies: clusters: general

1. Introduction

Galaxy clusters are the largest virialized structures in the Universe. The study of their abundance as a function of redshift can impose important constraints on the linear amplitude of mass fluctuations (Bahcall & Fan 1998). To find the number of clusters in any given redshift interval, one needs to know their commoving density $n(z)$. This may be predicted using the semi-analytic formalism of Press & Schechter (1974). In this model (and most of its variants) the space density of a given type of object exponentially depends on the rms dispersion in mass, σ_M, and also on the growth factor for the linear perturbation, $D(z)$. In the case of rich galaxy clusters, the linearized Abell radius (1.5 h^{-1} Mpc) is $\sim 8h^{-1}$ Mpc and, hence, σ_M on this scale can be determined from the observational abundance of these objects, becoming the so-called σ_8 parameter. The exponential dependence in the PS formula comes from the underlying hypothesis of a Gaussian distribution for the density fluctuations field. Such a dependence can be more or less intense if this distribution is not Gaussian. Clusters correspond to rare peaks in the density field and, as a consequence, any positive skewness in the probability density function, with respect to the Gaussian distribution, yields more clusters at higher redshifts. Some authors show that the mere observation of a few clusters at high redshifts could indicate a small level of non-Gaussianity in the primordial density field (e.g. Ribeiro et al. 2000 – RWL, Robinson & Baker 2000; Matarrese et al. 2000; Willick 2000).

Recent observations suggest the existence of clusters or protoclusters at relatively high redshifts. Some examples are the high-z quasar clustering evidence at $z \gtrsim 4$ (Djorgovski 1999; Steidel et al. 1998, 2005); Ly-α and LBG objects in the range $2 \lesssim z \lesssim 5$ (Röttgering et al. 2004; Pentericci et al. 2000); X-ray clusters from Chandra + XMM-Newton survey presenting high correlation length at $z \approx 1$ (Rosati et al. 2004). All these observations have some difficulties for any hierarchical structure formation model based on a strictly Gaussian statistics. Nevertheless, any level of non-Gaussianity (if present) should respect the severe constraints on CMB scales from recent WMAP data (e.g. Komatsu et al. 2003); non-Gaussian traces have already been detected in WMAP-1 and WMAP-3 year data (e.g. Chiang et al. 2006; Cruz et al. 2006; Vielva et al. 2004). These results have stimulated the investigation of non-Gaussian contributions using several kinds of models (e.g. Lyth 2006; Seery & Lidsey 2006; Allen et al. 2006). Some authors consider the possibility that non-Gaussianity is a scale-dependent feature and thus models in this context could fit both CMB and high-z galaxy clustering in the Universe (e.g. Andrade et al. 2004, 2005 – AWR04 and AWR05; Avelino & Liddle 2004; Mathis et al. 2004). In this work, continuing the studies of RWL, AWR04 and AWR05, we investigate the predictions of scale-dependent mixed non-Gaussian cosmological density fields for the space number density of massive galaxy clusters. Our aim is to use the current observational values of σ_8 in conjunction with high-z galaxy

clustering data to constrain the level of non-Gaussianity in the density field.

2. Structure formation

In this section, we briefly review the basics of Gaussian random fields and the PS formalism for the mass function.

2.1. Smoothed Gaussian random field

In a linear approximation, the theory of structure formation describes the evolution of the density contrast

$$\delta(\boldsymbol{x}) = \frac{\rho(\boldsymbol{x}) - \bar{\rho}}{\bar{\rho}}, \tag{1}$$

where $\rho(\boldsymbol{x})$ is the density at the point $\boldsymbol{x}$ and $\bar{\rho}$ is the cosmic mean density. The Fourier mode of the density contrast, $\delta_{\boldsymbol{k}}$, is given by

$$\delta_{\boldsymbol{k}} = \int \delta(\boldsymbol{x}) \mathrm{e}^{\mathrm{i}\boldsymbol{k}\cdot\boldsymbol{x}}\, \mathrm{d}\boldsymbol{x}. \tag{2}$$

The density contrast is smoothed by a window function $W(r)$ with a smoothing mass-scale M,

$$\delta_M(\boldsymbol{x}) \equiv \int W(|\boldsymbol{x}' - \boldsymbol{x}|)\delta(\boldsymbol{x}')\, \mathrm{d}\boldsymbol{x}' \tag{3}$$

or

$$\delta_M(\boldsymbol{x}) = \frac{1}{(2\pi)^3} \int \tilde{W}(kR)\delta_{\boldsymbol{k}} \mathrm{e}^{-\mathrm{i}\boldsymbol{k}\cdot\boldsymbol{x}}\, \mathrm{d}\boldsymbol{k} \tag{4}$$

where $\tilde{W}(kR)$ is the Fourier transform of the window function $W(r)$, R is a scale related to the mass M, and $k \equiv |\boldsymbol{k}|$.

The density field variance with a smoothing mass-scale M is

$$\sigma_M^2 \equiv \langle \delta_M^2 \rangle = \frac{1}{2\pi^2} \int \tilde{W}^2(kR) P(k) k^2\, \mathrm{d}k \tag{5}$$

where we have defined the power spectrum $P(k) \equiv \langle |\delta_{\boldsymbol{k}}|^2 \rangle$. The use of a spherical Heaviside function

$$W(r) = \frac{3}{4\pi R^3} \theta\left(1 - \frac{r}{R}\right) \tag{6}$$

or

$$\tilde{W}(kR) = \frac{3}{(kR)^3}(\sin kR - kR \cos kR), \tag{7}$$

with commoving scale $8\,h^{-1}$ Mpc, defines the usual measure of the linearly evolved power spectrum amplitude, σ_8, with corresponding mass $M_8 = 1.785(\Omega_m/0.3)\times 10^{14}\, h^{-1}\, M_\odot$, i.e., a typical galaxy cluster mass.

2.2. The mass function

To find the number of clusters of mass M in any given redshift interval, one needs to know their commoving density, $n(M, z)$. This may be predicted using the semi-analytic formalism of Press & Schechter (1974), where the basic assumption is that the amplitude of the primordial density fluctuations can be described by a Gaussian distribution:

$$P(\delta) = \frac{1}{\sqrt{2\pi}\sigma_M} \exp\left[-\frac{\delta^2}{2\sigma_M^2}\right]. \tag{8}$$

For fluctuations of a given mass M, the fraction $F(M)$ of those that become bound at a particular epoch are those with amplitudes greater than δ_c

$$F(M) = \frac{1}{\sqrt{2\pi}\sigma_M} \int_{\delta_c}^{\infty} \exp\left[-\frac{\delta^2}{2\sigma_M^2}\right] \mathrm{d}\delta, \tag{9}$$

where $\delta_c \approx 1.68$ is the linear threshold overdensity for collapse. This leads to the commoving number density of bound objects with mass in the range M and $M + \mathrm{d}M$:

$$\frac{\mathrm{d}n}{\mathrm{d}M} = \sqrt{\frac{2}{\pi}} \frac{\bar{\rho}}{M} \frac{\delta_c}{D(z)} \left(\frac{1}{\sigma_M^2}\right) \exp\left[-\frac{\delta_c^2}{2\sigma_M^2 D^2(z)}\right]. \tag{10}$$

3. Non-Gaussian random fields

The most accepted model for structure formation assumes initial quantum fluctuations created during inflation and amplified by gravitational effects. The standard inflation model predicts an adiabatic uncorrelated random field with a nearly flat, scale invariant spectrum on scales larger than $\sim 1^\circ$–2° (e.g. Bardeen et al. 1983). Simple inflationary models also predict that the density random field follows a nearly Gaussian distribution, where only small deviations from Gaussianity are allowed (e.g. Gangui et al. 1994). Actually, current data cannot disprove a small level of non-Gaussianity in the anisotropy of the cosmic background radiation temperature (e.g. Chiang et al. 2003).

Non-Gaussianity, even at a small level, implies an infinite range of possible statistical models. The general procedure for creating a wide class of non-Gaussian models is to introduce an operator that transforms Gaussianity into non-Gaussianity according to a specific rule. For instance, we can define a zero-mean random field ψ that follows a local transformation F on an underlying Gaussian field:

$$\psi(\boldsymbol{x}) = F(\phi) \equiv \alpha\phi(\boldsymbol{x}) + \epsilon\left[\phi^2(\boldsymbol{x}) - \langle \phi^2(\boldsymbol{x}) \rangle\right] \tag{11}$$

where α and ϵ are free parameters of the model. The field described by ψ is physically motivated in the context of non-standard inflation models (see e.g. Gangui et al. 1994). $P(\phi)$ is Gaussian, while $P(\psi) = \int W(\psi|\phi)P(\phi)\, \mathrm{d}\phi$, in which $W(\psi|\phi)$ is the transition probability from ϕ to ψ (e.g. Taylor & Watts 2000; Matarrese et al. 2000). An alternative way to introduce non-Gaussianity is that proposed by RWL, in which the PDF of ψ is directly modified as a mixture: $P(\psi) = (1 - \alpha) f_1(\phi) + \alpha f_2(\phi)$, where f_1 is the (dominant) Gaussian PDF and $f_2(\phi)$ modulates the shape of the resulting (slightly) non-Gaussian distribution, for small values of α. The particular choice of RWL was to define f_2 as a lognormal distribution. This choice is supported by the simple argument that the real PDF of the density field cannot be strongly non-Gaussian at CMB scales (see e.g. Stompor et al. 2001; Komatsu et al. 2003) and, at the same time, it should be approximately lognormal at galaxy cluster scales (see e.g. Plionis & Valdarnini 1995). Actually, as shown by AWR04, the choice of the second component in the mixed field is less important than the cross-correlation between the amplitude of both fields. According to RWL, α is a function of time that turns a nearly Gaussian PDF at recombination ($\alpha \approx 0$) into a nearly lognormal distribution ($\alpha \approx 1$) over the nonlinear regime, mostly at galaxy cluster scales. In this paper we consider the case where the seeds for structure formation are a weighted combination of adiabatic perturbations produced during inflation and active isocurvature perturbations produced by topological defects generated at the end of the inflationary epoch (see e.g. Battye & Weller 1998).

4. Structure formation in the mixed model

In the mixed scenario, we suppose that the field has a probability density function of the form:

$$\mathcal{P}[\delta_k] \propto (1-\alpha)f_1(\delta_k) + \alpha f_2(\delta_k). \quad (12)$$

The first field is the Gaussian component and the effect of the second component is to modify the Gaussian field to have a positive tail. The parameter α in (1) allows us to modulate the contribution of each component to the resultant field. Like the hybrid inflation models (Battye & Weller 1998; Battye et al. 1999), the mixture models consider the scenario in which structure is formed by both adiabatic density fluctuations produced during inflation and active isocurvature perturbations created by cosmic defects during a phase transition which marks the end of inflationary epoch.

Nevertheless, the mixed scenario just considers the correlation between the adiabatic and the isocurvature fields in the post-inflation Universe. So, the fluctuations in super-horizon scales (inflated during the exponential expansion) are strictly uncorrelated and the mixing effect acts only inside the Hubble horizon, on sub-degree scales. To allow for this condition and to keep a continuous mixed field, a scale dependent mixture parameter, $\alpha \equiv \alpha(k)$ was defined. We assume the simplest choice of $\alpha(k)$, a linear function of k:

$$\alpha(k) \equiv \alpha_0 k. \quad (13)$$

4.1. The mixed power spectrum

To constrain the two component random field, we take $\delta_k = P(k)\nu^2$, where ν is a random number with a distribution given by (12). So, we consider the primordial power spectrum of the mixed field in the form:

$$P(k)^{\rm mix} \equiv \mathcal{M}^{\rm mix}(\alpha_0, k)P(k) \quad (14)$$

where the $P(k)$ is the primordial power-law spectrum and $\mathcal{M}^{\rm mix}(\alpha_0, k)$ is the mixture term, a functional of f_1 and f_2, which accounts for the statistical effect of the new component:

$$\mathcal{M}^{\rm mix}(\alpha_0, k) \equiv \int_\nu [(1-\alpha_0 k)f_1(\nu) + \alpha_0 k f_2(\nu)]\nu^2 \, {\rm d}\nu. \quad (15)$$

In the case of a pure Gaussian field, $\alpha_0 = 0$, $\mathcal{M}^{\rm mix}(\alpha_0, k) = 1$, and the power spectrum is just the simple power-law spectrum, k^n, where n is the spectral index predicted by inflationary models. In the case of a mixed field, correlations between both fields are estimated by the integral in Eq. (15), on mixture scales defined by Eq. (13). Introducing the Gaussian+lognormal mixture distribution in (15), we have the following integral for the mixture term

$$\mathcal{M}^{\rm mix}(\alpha_0, k) = \int_\nu \left[\frac{(1-\alpha_0 k)}{\sqrt{2\pi}} {\rm e}^{-\nu^2/2} + \frac{\alpha_0 k}{\nu\sqrt{2\pi}} {\rm e}^{-(\ln\nu)^2/2}\right] \nu^2 \, {\rm d}\nu. \quad (16)$$

Solving this integral we find

$$\mathcal{M}^{\rm mix}(\alpha_0, k) = 1 + \alpha_0 k \left(\frac{e^2}{2} - 1\right) > 1, \quad (17)$$

and hence the contribution of $\mathcal{M}^{\rm mix}(\alpha_0, k)$ to the power spectrum is always positive. The overall effect, however, also depends on the mixed transfer function estimated according to

$$T^2_{\rm mix}(k) \equiv (1-\alpha_0 k)^2 T^2_{\rm adi}(k) + 2(1-\alpha_0 k)(\alpha_0 k) T_{\rm adi}(k) \times T_{\rm iso}(k) + (\alpha_0 k)^2 T^2_{\rm iso}(k) \quad (18)$$

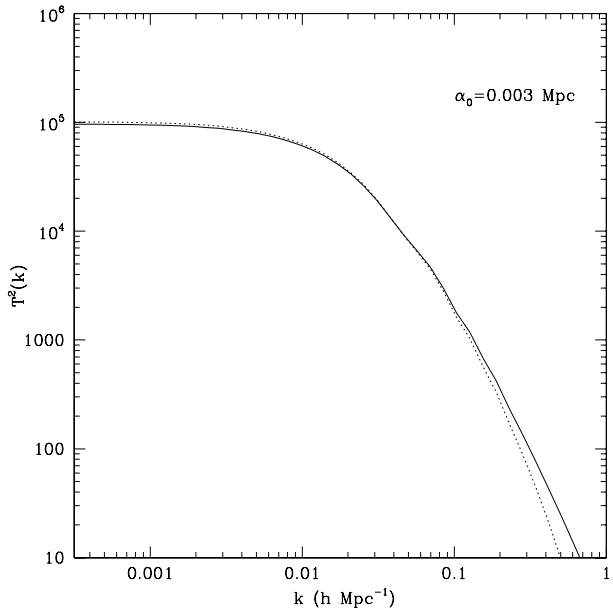

Fig. 1. Transfer function of matter: the solid line is the adiabatic case, the dotted line is the mixed case for a lognormal with $\alpha_0 = 0.003$ Mpc.

where $T_{\rm adi}(k)$ and $T_{\rm iso}(k)$ are the transfer functions computed by CMBFAST (Seljak & Zaldarriaga 1996) for adiabatic and isocurvature seed initial conditions, respectively. Although an isocurvature transfer function is not a necessary condition for mixed models, we have assumed such a feature here in order to be consistent with our previous work (AWR04 and AWR05).

To see the total influence of the second component, we compute the power spectrum of matter as

$$P^{\rm mix}(k) = 2\pi^2 \delta_H^2 \frac{k^n}{H_0^{n+3}} T^2_{\rm mix}(k)\mathcal{M}^{\rm mix}(\alpha_0, k) \quad (19)$$

where $\delta_H \simeq 1.9 \times 10^{-5}$, $H_0 = 100\,h^{-1}\,{\rm km\ s^{-1}\ Mpc^{-1}}$ (e.g. Dodelson 2003).

In Fig. 1, we compare the mixed transfer function with the strict adiabatic case. In this plot, the choice of $\alpha_0 = 0.003$ Mpc corresponds to the maximum value for this parameter to be consistent with the CMBR anisotropies (see AWR04). This scale, at recombination, corresponds to the commoving length scale of $10^{12}\ M_\odot$ (the baryonic damping mass by photon diffusion) and should be equivalent to the minimal value of α_0 for later times of the structure formation process. Note in this figure that the effect of the mixed field is a power transfer from smaller scales to larger physical scales, the critical point being $k \simeq 0.04\ h\ {\rm Mpc^{-1}}$ (the pure effect of $T^2_{\rm mix}(k)$). This point is displaced to $k \simeq 0.45\ h\ {\rm Mpc^{-1}}$ when we compute the power spectrum, as we can see in Fig. 2 (resulting from the combined effect of $T^2_{\rm mix}(k)$ and $\mathcal{M}^{\rm mix}(\alpha_0, k)$). Hence, the distinctive feature of the mixed model is the prediction of less power at galaxy scales and slightly more power at larger scales.

4.2. Mass variance in the mixed model

We estimate the mass variance as a function of α_0 using

$$\sigma_8^2(\alpha_0) = \frac{1}{2\pi^2} \int \tilde{W}^2(k8h^{-1})P(k)^{\rm mix}k^2 \, {\rm d}k. \quad (20)$$

Solving this integral for increasing values of α_0, with the following set of parameters: $\Omega_m = 0.27$, $\Omega_\Lambda = 0.73$, $h = 0.7$ and

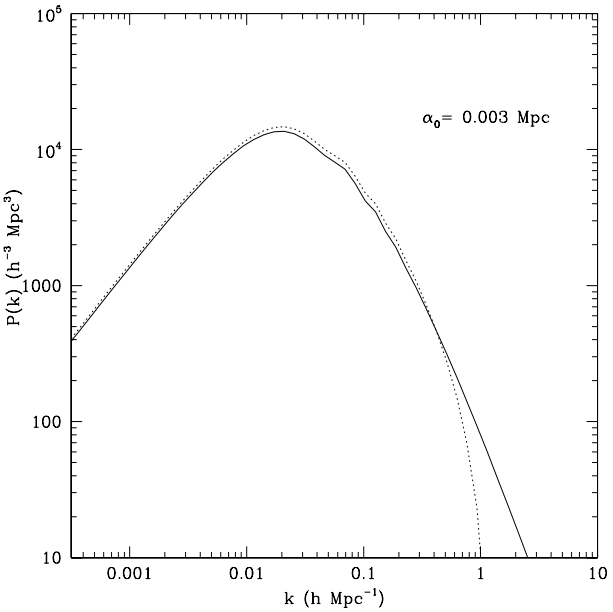

Fig. 2. Power spectrum of matter: the solid line is the Gaussian case, the dotted line is the mixed case for a lognormal with $\alpha_0 = 0.003$ Mpc.

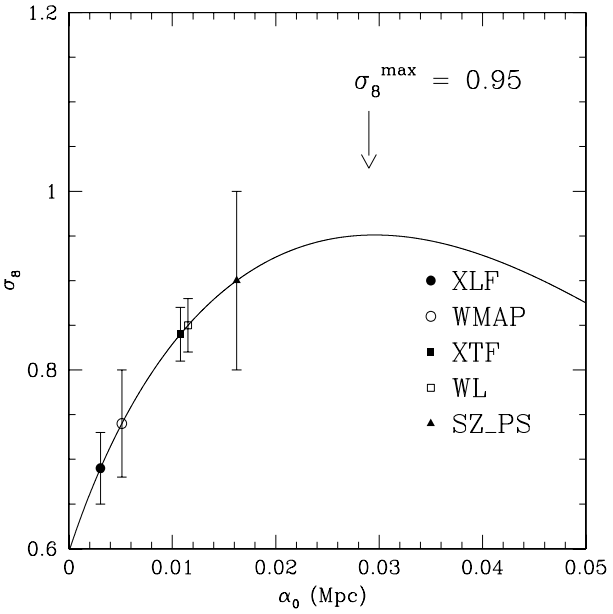

Fig. 3. σ_8 as a function of α_0. The data points projected onto the curve are: XLF and XTF (X-ray luminosity and temperature functions), WL (weak lensing), SZ PS (Sunyaev-Zeldovich effect power spectrum) and WMAP (Wilkinson Microwave Anisotropy Probe).

$n = 0.96$ (Spergel et al. 2003), we find the behavior presented in Fig. 3, where we also plot some data points on the theoretical curve in order to set observational constraints to the model. The estimates of σ_8 are based on different methods and were taken from the compilation of Pierpaoli et al. (2003). The data suggest that the value of σ_8 is approximately in the range 0.7–0.9, which corresponds to the range 0.001–0.01 Mpc for α_0. The presence of a maximum value of $\sigma_8 \simeq 0.95$ corresponding to $\alpha_0 \simeq 0.03$ Mpc is seen. This is the scale where the mixed transfer function becomes dominated by the contribution of small scales ($k \to \infty$) in integral (20). This is an interesting feature of the model, being directly related to the way we define $T^2_{\rm mix}(k)$ in Eq. (18).

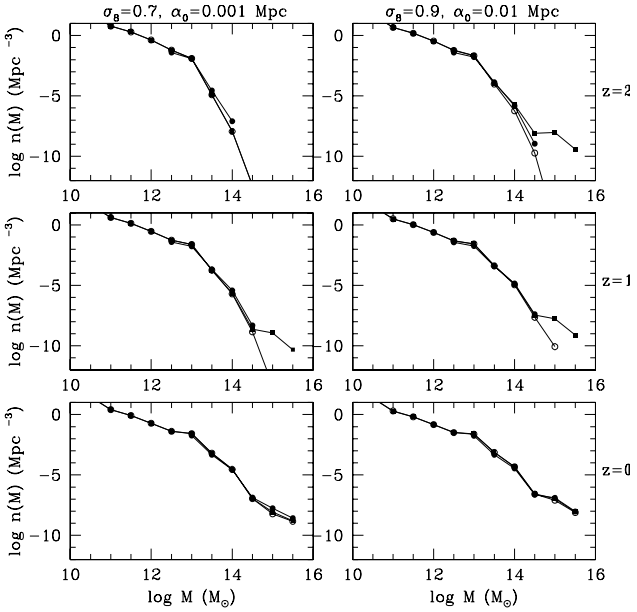

Fig. 4. Comparison between mass functions following J01, PSG and PSNG. Filled circles are J01; open circles are PSG; and filled squares are PSNG. Power spectra built from CMBFAST transfer function.

4.3. Mass function of massive clusters

By modifying the original PS formula to take into account the small non-Gaussianity, we rewrite Eq. (10) as a function of σ_M

$$f(\sigma_M^{-1}) = \sqrt{\frac{2}{\pi}}\left[(1-\alpha_0)(\delta_c\sigma_M^{-1})\exp\left(-(\delta_c\sigma_M^{-1})^2/2\right)\right] + \sqrt{\frac{2}{\pi}}\left[\frac{\alpha_0}{2}(\ln\delta_c\sigma_M^{-1})\exp\left(-(\ln\delta_c\sigma_M^{-1})^2/2\right)\right]. \quad (21)$$

The result is presented in Figs. 4 and 5, where we compare our model with the standard PS (just the first term of Eq. (21)) and also with the fitting formula obtained from the Virgo Consortium Cluster Data by Jenkins et al. (2001)

$$f(\ln\sigma_M^{-1}) = A\exp\left[-|\ln\sigma_M^{-1} + B|^\epsilon\right] \quad (22)$$

where the parameter B controls the location of the peak in the collapsed mass fraction, A controls the overall mass fraction in halos and ϵ stretches the function to fit the overall shape of the simulations (in this work we follow Jenkins et al. 2001 and set $A = 0.315$, $B = 0.61$ and $\epsilon = 3.8$). In Fig. 4, all the spectra are built from the CMBFAST transfer function: pure adiabatic for Gaussian and mixed for non-Gaussian models. We verify a higher density of objects with $M > 10^{14}\ M_\odot$ at high redshifts in comparison with the strictly Gaussian case. This result is similar to others found in different works dealing with non-Gaussianity (e.g. Amara & Refregier 2003; Mathis et al. 2004).

This effect is even clearer if we integrate Eq. (21) for $M > 8.0 \times 10^{14}\ M_\odot$, thus finding the abundance as a function of the redshift: $n(z)$. The result is presented in Fig. 5, where we also depict a possible scenario of galaxy cluster formation based on observational evidence of high-z galaxy clustering in the Universe. In this figure we see a vertical line indicating the redshift up to which galaxy clusters are detected in the Chandra + XMM-Newton experiments (Rosati et al. 2004); and regions where we find observations of high-z galaxy clustering, Ly-α and LBG objects at $z \gtrsim 2$ (Röttgering et al. 2003; Pentericci et al. 2000) and

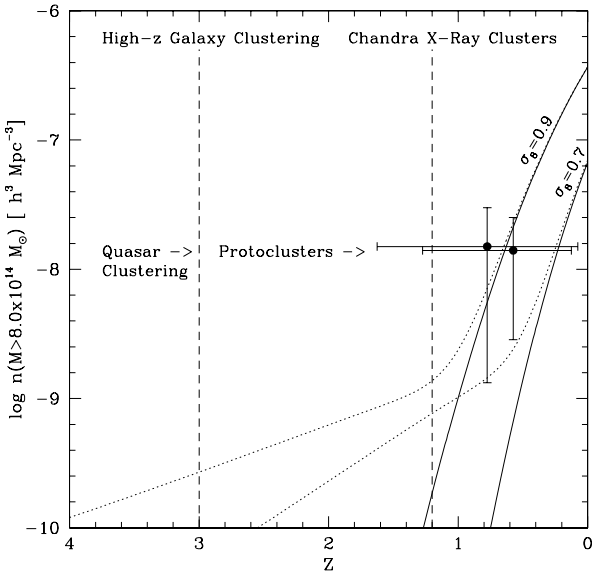

Fig. 5. Galaxy cluster evolution scenario at high redshifts. Data points correspond to the most massive EMSS clusters. Possible formation sequence: 1°) quasar clustering at first stage ($z \lesssim 4-5$); then 2°) normal galaxy clustering – the protocluster stage ($z \lesssim 3-4$) and 3°) virialized clusters ($z \lesssim 1-2$).

quasars at $z \gtrsim 4$ (Djorgovski 1999; Steidel et al. 1998, 2005). It is important to note in this figure the degeneracy between σ_8 and α_0 for $z \gtrsim 1$, which implies the need for well selected samples of galaxy clusters at these redshifts in order to distinguish between Gaussian and nearly-Gaussian initial conditions.

5. Discussion

Continuing the work of RWL, AWR04 and AWR05, we explore the effects of small non-Gaussianities, defined by a mixed distribution model, on the mass variance at galaxy cluster scale. The mixed power spectrum and the $\sigma_8 - \alpha_0$ relation were obtained from a finite mixture model according to RWL, with a weighted adiabatic and isocurvature transfer function. Observational data on σ_8 allowed us to constrain the mixture parameter to $0.001 \lesssim \alpha_0 \lesssim 0.01$ Mpc. If we take this in conjunction with the result of AWR04, $\alpha_0 \lesssim 0.003$ Mpc in order for the model to be consistent with the CMBR anisotropies, we are led to a very restricted range for the mixture parameter: 0.001–0.003 Mpc. As a consequence, we have $\sigma_8 \simeq 0.7-0.74$.

Using the extreme values for α_0 (one for each value of σ_8, and relaxing the upper limit set by AWR04 in the case of $\sigma_8 = 0.9$), we estimate the effects of such small Gaussian deviations on the number density evolution of galaxy clusters. Our results suggest a scenario where structures develop earlier in comparison to strictly Gaussian models due to the mass function dependence on the mixture parameter α_0 and the lognormal component (the positive skewness effect).

The evolution of cluster abundance with redshift also indicates the need for well selected cluster samples around $z \gtrsim 1$ to discriminate between Gaussian and non-Gaussian (mixed) distribution models. Although the available data are not complete up to such redshifts, current (and future) observational missions will probably allow us to answer this question. For the moment, we conclude that the observational evidence for earlier stages of galaxy cluster formation since $z \approx 5$ marginally favors models with a small level of non-Gaussianity. The question of possible effects of dark energy on our present results will be probed in future work.

Acknowledgements. We thank the anonymous referee and C. A. Wuensche for useful suggestions. This work has the financial support of CNPq (grants 470185/2003-1 and 306843/2004-8) and UESC (grant 220.1300.357). A.P.A.A. also acknowledges the financial support of CNPq and FAPESB, under grant 1431030005400. C.M.C. acknowledges the fellowship from CAPES.

References

Allen, L., Gupta, S., & Wands, D. 2006, JCAP, 01, 06
Amara, A., & Refregier, A. 2004, MNRAS, 351, 375
Andrade, A. P. A., Wuensche, C. A., & Ribeiro, A. L. B. 2004, ApJ, 602, 555
Andrade, A. P. A., Wuensche, C. A., & Ribeiro, A. L. B. 2005, Phys. Rev. D, 71, 043501
Avelino, P., & Liddle, A. 2004, MNRAS, 348, 105
Bahcall, N., & Fan, X. 1998, ApJ, 504, 1
Bahcall, N., & Bode, P. 2003, ApJ, 588, 1
Bardeen, J. M., Steinhardt, P. J., & Turner, M. S. 1983, Phys. Rev. D, 28, 679
Battye, R., & Weller, J. 1998, in Relativistic Astrophisics and Cosmology, 164
Chiang, L., Naselsky, P., Verkhodanov, O., & Way, M. 2003, ApJ, 590, L65
Chiang, L., Naselsky, P., & Coles, P. 2006, ApJ [arXiv:astro-ph/0603662]
Cruz, M., Cayon, L., Martinez-Gonzalez, E., Vielva, P., & Jin, J. 2006, ApJ [arXiv:astro-ph/0603859]
Djorgovski, G. 1999, in The Hy-Redshift Universe: Galaxy Formation and Evolution at High Redshift, ASP Conf. Proc., 193, 397
Dodelson, S. 2003, Modern Cosmology (Academic Press)
Gangui, A., Lucchin, F., Matarrese, S., & Mollerach, S. 1994, ApJ, 501, L1
Jenkins, A., Frenk, C., White, S., et al. 2001, MNRAS, 321, 372
Komatsu, E., Kogut, A., Nolta, M. R., et al. 2003, ApJ, 148, 119
Lyth, D. 2006, JCAP, 06, 015
Matarrese, S., Verde, L., & Jimenez, R. 2000, ApJ, 541, 10
Mathis, H. Diego, J., & Silk, J. 2004, MNRAS, 353, 681
Pentericci, L., Kurk, J., Röttgering, H., et al. 2000, A&A, 361, L25
Pierpaoli, E., Borgani, S., Scott, D., & White, M. 2003, MNRAS, 325, 77
Plionis, M., & Valdarnini, R. 1995, MNRAS, 272, 869
Press, W., & Schechter, P. 1974, ApJ, 187, 425
Ribeiro, A. L. B. Wuensche, C. A., & Letelier, P. 2000, ApJ, 539, 1
Robinson, J., & Baker, J. 2000, MNRAS, 311, 781
Rosati, P., Tozzi, P., Ettori, S., et al. 2004, AJ, 127, 230
Röttgering, H., Daddi, E., Overzier, R., & Wilman, R. 2003, New Astron. Rev., 47, 309
Seljak, U., & Zaldarriaga, M. 1996, ApJ, 469, 437
Seery, D., & James, L. 2006, JCAP, 06, 01
Spergel, D. N., Verde, L., Peiris, H. V., et al. 2003, ApJS, 148, 175
Steidel, C., Adelberger, K., Dickinson, M., et al. 1998, ApJ, 492, 428
Steidel, C., Adelberger, K., Shapley, A., et al. 2005, ApJ, 626, 44
Stompor, R., Abroe, M., Ade, P., et al. 2001, ApJ, 561, L7
Taylor, A., & Watts, P. 2000, MNRAS, 314, 92
Vielva, P., Martinez-Gonzalez, E., & Vanderghenynst, P. 2004, ApJ, 609, 22
Willick, J. 2000, ApJ, 530, 88